

Electronic Supplementary Information

Tackling elemental mercury removal from wet-gas phase by enhancing the performance of redox active copper based adsorbents utilising operando pre-heating system

Syamzari Rafeen^{*a}, Rafin Ramli^a and Geetha Srinivasan^{*a,b}

^aPETRONAS Research Sdn. Bhd., Lot 3288 & 3289, Off Jalan Ayer Itam, Kawasan Institusi Bangi, 43000 Kajang, Selangor, Malaysia

^bQUILL, The Queen's University of Belfast, Belfast, BT9 5AG, UK

Materials

Ionic liquid (IL), 1-butyl-3-methylimidazole chloride ([C₄mim]Cl) was synthesised at QUILL. It was chemically pure by NMR and with <100 ppm of water.

[C₄mim]Cl

¹H NMR (CDCl₃): δ 10.83 (s, 1H), 7.30 (s, 1H), 7.22 (s, 1H), 4.26 (t, J=7.3 Hz, 2H), 4.06 (s, 3H), 1.88-1.76 (m, 2H), 1.42-1.22 (m, 2H), 0.90 (t, J=7.3 Hz, 3H).

¹³C NMR (CDCl₃): δ 137.82, 124.11, 122.44, 49.89, 36.70, 32.37, 19.63, 13.64.

Preparation of solid-supported adsorbent and performance testing

Synthesised samples with its microanalysis results

1. CuCl₂ impregnated on silica JM6 (from Johnsons Matthey): % experimental (% calculated):
Cu 1.70 (2.00), Cl 2.10 (2.23)
2. NaCl-CuCl₂ impregnated on silica JM6, $\chi_{\text{CuCl}_2} = 0.5$
Cu 1.60 (2.00), Na 0.85 (0.72), Cl 2.70 (3.35)
3. [C₄mim]Cl-CuCl₂ impregnated on silica JM6, $\chi_{\text{CuCl}_2} = 0.5$
Cu 1.90 (2.00), C 2.99 (3.02), H <0.30 (0.47), N <0.30 (0.88), Cl 3.22 (3.35)
4. NaCl (2 wt% Na) impregnated on silica JM6, $\chi_{\text{CuCl}_2} = 0$
Na 2.17 (2.00), Cl 2.93 (3.09)
5. NaCl-CuCl₂ impregnated on silica JM6, $\chi_{\text{CuCl}_2} = 0.67$
Cu 1.70 (2.00), Na 0.55 (0.36), Cl 2.21 (2.79)

6. NaCl-CuCl₂ impregnated on activated carbon WS490 (from Calgon), $\chi_{\text{CuCl}_2} = 0.5$
Cu 1.70 (2.00), Na 0.57 (0.72), Cl 3.34 (3.35)
7. CuCl₂ impregnated on activated carbon WS490, $\chi_{\text{CuCl}_2} = 1$
Cu 2.00 (2.00), Cl 2.56 (2.23)
8. [C₄mim]Cl-CuCl₂ impregnated on γ -alumina, $\chi_{\text{CuCl}_2} = 0.5$
Cu 2.20 (2.00), C 3.14 (3.02), H 0.38 (0.47), N 1.03 (0.88), Cl 3.27 (3.35)
9. NaCl-CuCl₂ impregnated on γ -alumina, $\chi_{\text{CuCl}_2} = 0.5$
Cu 1.80 (2.00), Na 0.74 (0.72), Cl 2.72 (3.35)

Analytical Results

Thermogravimetric Analysis (TGA)

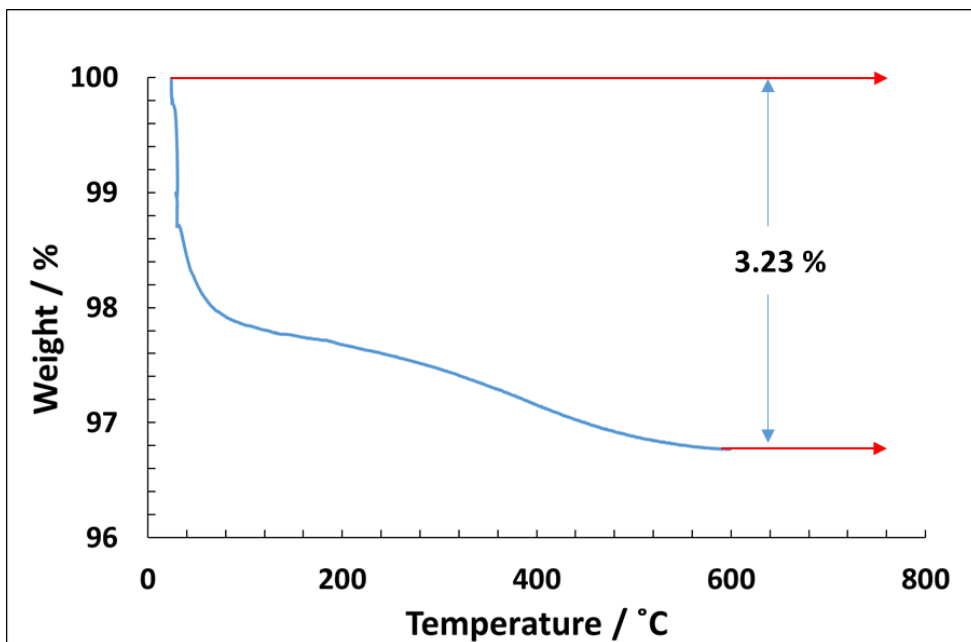


Figure 1: TGA analysis for blank silica shows an overall weight loss of 3.23 wt% where about 2% below 150 °C and about 1.23% is lost between 200 °C and 600 °C.. The loss below 150 °C can be ascribed to the weakly bound water on the silica surface, whilst above 200 °C can be attributed to the dehydroxylation of the silica surface.

Scanning Electron Microscopy – Energy Dispersive X-Ray (SEM-EDX)

The scanning electron microscopy (SEM) micrograph and the corresponding EDX spectra for CuCl₂/SiO₂ (Figure 2) show good dispersion of CuCl₂ on the surface of the support. The blue dots on the EDX map, representing copper element were well dispersed, and demonstrated close association with the yellow dots representing chlorine sites. A simple visual estimation suggests that the chlorine is present in higher

concentration than copper, corresponding to the atomic ratio of copper(II) chloride. The image also indicates no cluster formation of CuCl_2 on the support. SEM/EDX results on selected adsorbent samples are presented here, however please note that based on the analyses conducted on all adsorbent samples showed uniform distribution of reactive chemicals across their surfaces.

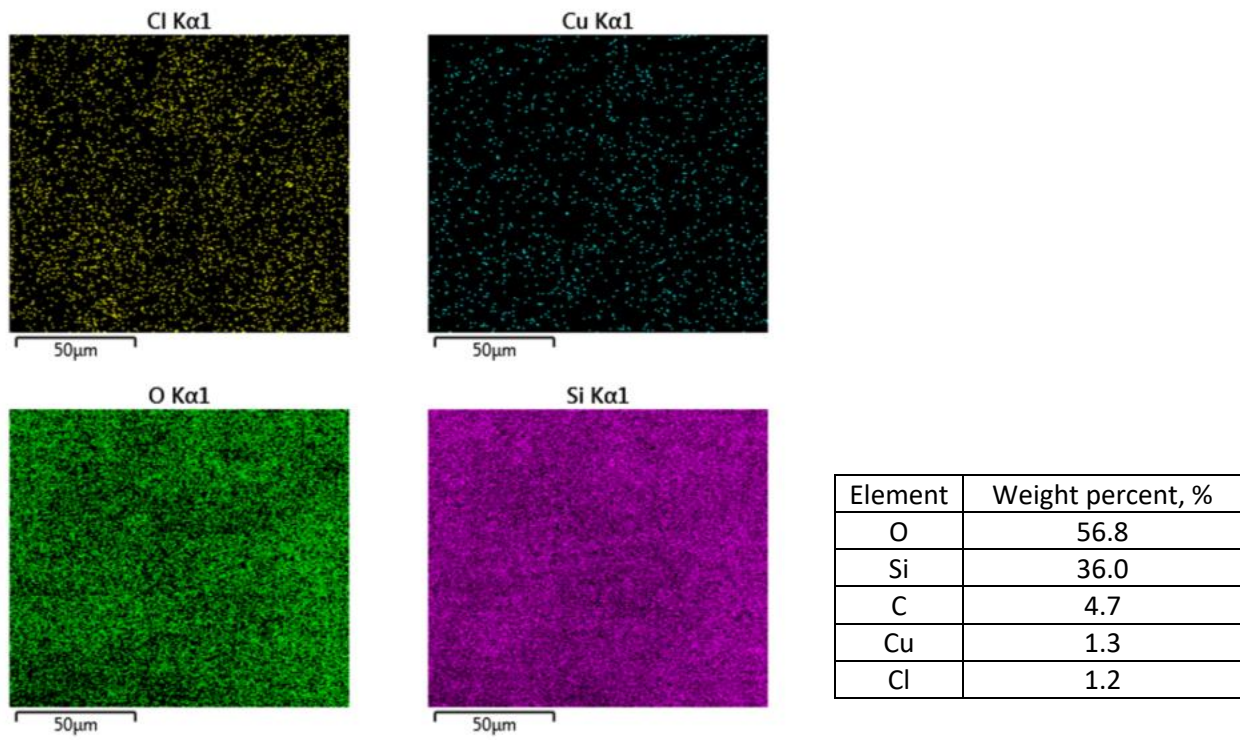


Figure 2 Scanning electron microscopy (SEM) micrograph and the corresponding elemental distribution for CuCl_2 on SiO_2 ; carbon from carbon sputtering for image clarity

Figure 3 shows the distribution of copper(II) chloride on silica in the presence of NaCl. The copper(II) surface coverage shows general uniformity with both Cu and Na occupying different spots on the support. The randomness of the elemental distribution *i.e.* Cl (blue), Cu (purple) and Na (yellow) indicated the lack of complex formation as a result of the mixture although no structural confirmation

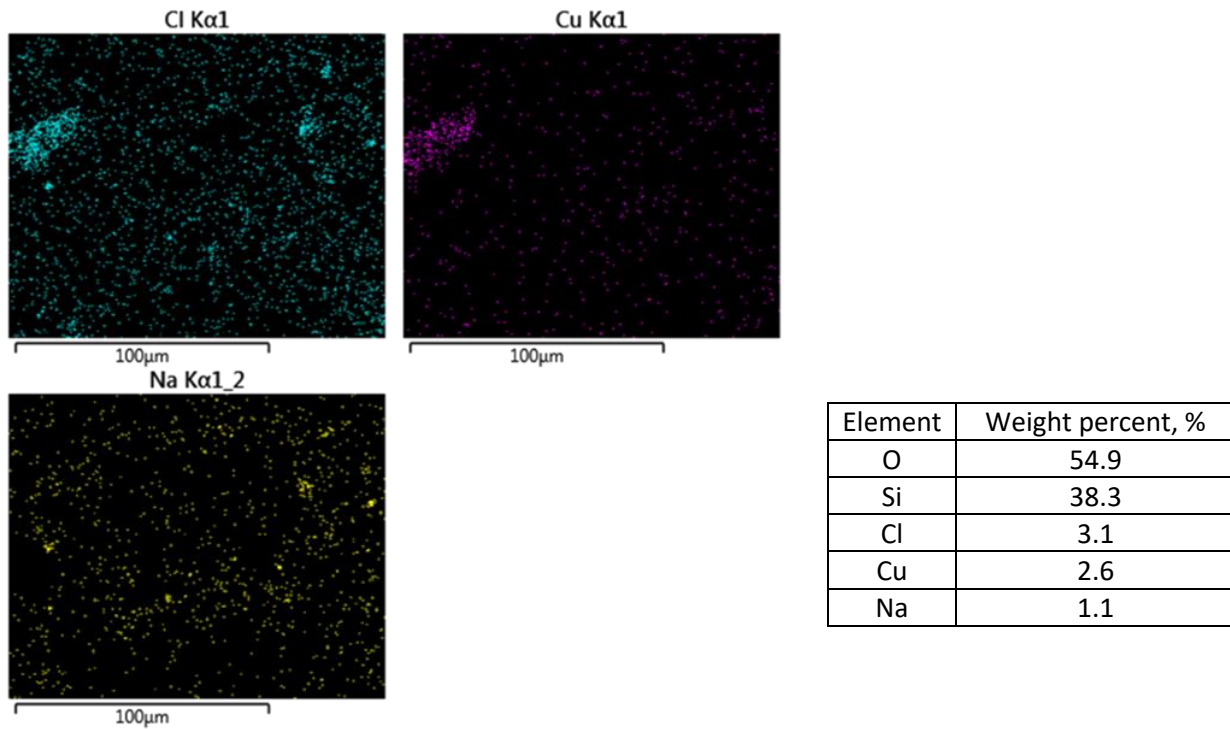


Figure 3: Scanning electron microscopy (SEM) micrograph and the corresponding elemental distribution for CuCl_2 and NaCl on SiO_2

Powder X-Ray Diffraction

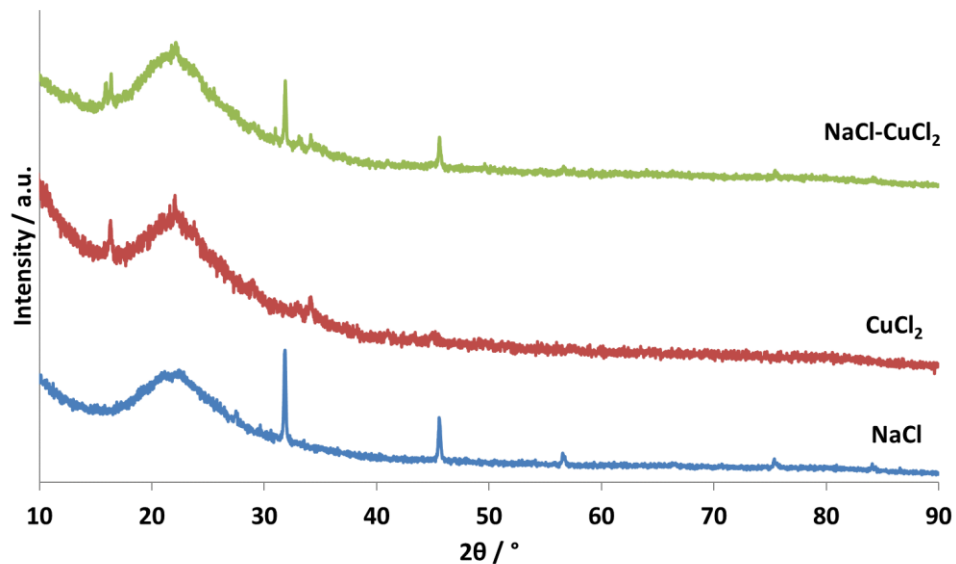


Figure 4: Powder X-Ray Diffraction patterns for silica-supported NaCl (total loading = 1.84 wt%), CuCl₂ (total loading = 4.23 wt%), and binary salt NaCl-CuCl₂, $\chi_{\text{CuCl}_2} = 0.50$ (total loading = 6.07 wt%)

The diffractogram of the supported NaCl-CuCl₂ $\chi_{\text{CuCl}_2} = 0.50$ system, showed the presence of characteristic peaks of both the NaCl and CuCl₂ precursors even at low salt loading (*i.e.* total loading = 6.07 wt%). The CuCl₂ diffraction was weak and poorly resolved in comparison with the bulk system, because it was only present at lower concentrations of 4.24 wt%. Nonetheless, there was no evidence to indicate the formation of a new phase between the NaCl and CuCl₂, in the presence or absence of the silica support.

Instrumentation

Mercury Analysis - PSA 10.525 Series Sir Galahad

The total mercury contents of samples measured for gas phase extraction were determined using a PSA 10.525 Series Sir Galahad mercury analyser. The Sir Galahad (SG) determines mercury concentration in wide range of gaseous media, including ambient air, natural gas and stack gases. Nitrogen gas was used for operating in safer conditions and it was proven to mimic natural gas in all our studies since 2006. The SG is based on atomic fluorescence, in conjunction with amalgamation in a gold trap in the detection system.

Microanalysis: Elemental and Halide Content

Elemental C, H, N, and S content in the samples were determined using Perkin-Elmer Series II CHNS/O 2400 CHN Elemental Analyser, which provided analytical results within an accuracy of 0.3 wt% of the theoretical values. For metal analysis, the samples were analysed using Agilent Technologies 5100 ICP-OES with an accuracy of 0.1 p.p.m. The halide content analysis was performed by oxygen flask combustion followed by a halide titration with mercury(II) nitrate, using a dicarbazide indicator. The detection level for this analysis was estimated to be ± 0.5 wt%.

UV-visible spectroscopy

Transmission mode

UV-visible–near-IR optical absorption spectra were measured on a Perkin Elmer Lambda 950 UV/vis spectrometer, controlled by Perkin Elmer UV Winlab software version 6.0.2.0723. Measurements were taken from 200 to 2000 nm in 1 mm and 0.01 mm quartz cuvettes (from Suprasil) at a scan speed of 215 nm min⁻¹.

The ‘detector change’ position was shifted from 860 nm to 500 nm to avoid any interference with the absorption bands for the d-d ligand field transition of samples being analysed (*i.e.* CuCl₂ in water).

Diffuse reflectance

The UV-visible spectra for the solid samples were measured on a Perkin Elmer Lambda 950 UV/vis spectrometer equipped with a diffuse reflectance accessory (from Praying Mantis), and the spectra were recorded in the range between 200 and 2000 nm. BaSO₄ was used as reference and the samples were set in holders with 2 mm thickness during measurements.

The ‘detector change’ position was shifted from 860 nm to 700 nm to avoid any interference with the absorption bands for the d-d ligand field transition of samples being analysed (*i.e.* CuCl₂.2H₂O).

Thermogravimetric Analysis (TGA)

Thermal decomposition profiles were collected by thermogravimetric analysis using a TA TGA Q5000 instrument with heating rate of 5 °C min⁻¹ under a dinitrogen environment.

Scanning Electron Microscopy-Energy Dispersive X-Ray Spectroscopy (SEM-EDX)

Topography and morphology characteristics were studied using a FEI Quanta FEG Scanning Electron Microscopy (SEM) attached with Energy Dispersive X-ray (EDX) spectrometer and Everhart Thornley Detector (ETD).

Surface Area and Porosity

The BET surface area and BJH Method to determine the Pore Volume and Pore Size data of the solid supports were performed using a Micromeritics ASAP 2020 Accelerated Surface Area and Porosimetry Analyser.